

ASSESSING THE GLOBAL AND ARCTIC TRANSPORT AND FATE OF POLYCHLORINATED BIPHENYLS USING THE ATMOSPHERIC CHEMICAL TRANSPORT MODEL GEOS-CHEM

Friedman CL^{1*}, Thackray C², Selin NE³

¹Center for Environmental Health Sciences, Massachusetts Institute of Technology, 77 Massachusetts Avenue, Cambridge, MA, USA

²Department of Earth, Atmospheric, and Planetary Sciences, 77 Massachusetts Avenue, Cambridge, MA, USA

³Engineering Systems Division and Department of Earth, Atmospheric, and Planetary Sciences, 77 Massachusetts Avenue, Cambridge, MA, USA

Introduction

Polychlorinated biphenyls (PCBs) are toxic, persistent, and bioaccumulative industrial chemicals whose production and use have been banned internationally via several multilateral environmental agreements, including the UNECE's Convention on Long Range Transboundary Air Pollution (CLRTAP) and the Stockholm Convention. Despite the ban, PCBs continue to cycle through the global atmosphere because of their persistence, passive emissions from remaining stocks, and release from natural storage reservoirs, such as oceans or soils. In particular, PCBs have been shown to transport long distances in the atmosphere to locations remote from their emissions, especially to the Arctic. The main mechanism for this transport is hypothesized to be the "grasshopper effect", whereby PCBs vaporize at warmer, lower latitudes, and then condense and deposit at higher, colder latitudes¹. While PCB emissions are low in Arctic latitudes, their efficient transport to and accumulation in the food web there causes adverse effects with multiple endpoints, and those affected receive few of the benefits of their industrial use. Adverse outcomes manifest as health risks to animals in the Arctic marine food web and to indigenous populations relying on traditional subsistence hunting practices for food.

Because of the potential for PCBs to accumulate in the Arctic and cause adverse effects, there have been a number of studies using models to investigate outstanding questions surrounding their emissions and environmental fate and transport. For example, Hung et al.² used the zonally-averaged model GLOBO-POP to investigate temporal trends of PCBs in the atmosphere in the Canadian Arctic and around the Great Lakes during the 1990s, and found that atmospheric concentration declines follow those of historical emissions, suggesting primary emissions (rather than re-emissions from other environmental media) are still the main factor controlling atmospheric levels. MacLeod et al.³ evaluated the multimedia model BETR-Global's ability to simulate atmospheric PCB concentrations against data from several observational networks in the northern hemisphere. Nearly all of the simulated data was within ten times measurements, and the model was used to demonstrate that the North Atlantic Oscillation can potentially impact atmospheric PCB concentrations by a factor of two. Gong et al.⁴ implemented a gas-particle partitioning scheme into the global 3-D GEM/POPs transport model, and compared simulated concentrations to data from networks measuring at high frequency in the northern hemisphere. While the model captured the relative differences among different PCB congeners, the authors concluded that the model was "semi-quantitative" due to uncertainties in emissions inventories, surface-air exchange, and lack of agreement in seasonal variations. Huang et al.⁵ also used the GEM/POPs model to investigate PCB global transport and budgets of the same three congeners. Major findings included determining that intercontinental transport in the northern hemisphere was seasonally-regulated, transport pathways from Europe and the North Atlantic contributed the greatest masses of PCBs to the Arctic, revolatilization from soil and water was a comparable source to anthropogenic emissions for CB28, and particle-associated PCBs reach higher levels in the atmosphere than gas phase PCBs.

Other studies have used models to predict how climate changes will impact atmospheric PCB transport. Lamon et al.⁶ examined the multimedia behavior of PCBs under future climate and found increased PCB volatilization and atmospheric transport driven mostly by rising temperatures. Ma and Cao⁷ developed an air-surface perturbation model to examine climate change effects on PCBs, also finding higher temperatures increase air concentrations. Ma et al.⁸ compared Arctic concentrations with simulations of the effect of climate change, finding that a wide range of POPs, including PCBs, have already been remobilized in the Arctic because of sea-

ice retreat and warming temperatures. Collectively, studies investigating PCB transport in a future climate suggest higher temperatures will induce higher primary and secondary emissions compared to today's climate, implying efforts to reduce PCB levels in the Arctic may be undermined.

Here, we modify the global chemical transport model GEOS-Chem to simulate atmospheric PCB transport and investigate the effects of predicted climate changes and declining primary emissions, especially on transport to the Arctic. GEOS-Chem simultaneously offers several advantages compared to other models, including global meteorological reanalysis input at fine spatial (4°x5°) and temporal (3 or 6 hour) scales, the ability to couple to climate predictions from general circulation models, interaction with spatially and temporally resolved simulated atmospheric particles and radicals, and surface-air exchange. Here, we aim to quantify changes in atmospheric concentrations of PCBs under 2050 climate, 2000 emissions ("FC"); 2000 climate, 2050 emissions ("FE"); and 2050 climate and emissions combined ("FCFE"); relative to a 2000 climate, 2000 emissions ("control") scenario, and determine the major processes affecting these changes.

Materials and methods

Model Description We use the chemical transport model GEOS-Chem⁹ (version 8-03-02) to simulate global atmospheric PCB transport in both the present and future. We simulate concentrations of two congeners: CB28 (2,4,4'-trichlorobiphenyl) and CB153 (2,2',4,4',5,5'-hexachlorobiphenyl), with the former more volatile than the latter. GEOS-Chem is also used to generate present and future concentrations of species interacting with PCBs; i.e., carbonaceous particles (CP) and hydroxyl radical (OH). The GEOS-Chem POPs model was developed and applied to PAHs by Friedman and Selin¹⁰, with updates in Friedman et al.¹¹. Here, we make several adaptations to the POPs model to address PCBs. In contrast to the PAH simulation, a lumped CP concentration is considered (given lack of evidence of stronger PCB partitioning to black carbon compared to organic carbon), with K_{OA} used to describe partitioning between the gas and particle phases. Oxidation by O₃ is also not considered because of lack of data demonstrating PCB particle phase oxidation. Monthly mean CP and OH concentrations are read into the PCB model at each time step. In the version of the PCB model presented here, only soil-atmosphere surface interactions are considered, so that initial results can be directly compared to PAH results¹¹, though future versions of the model will include interaction with other surface media, including water (oceans and lakes), vegetation, and snow. PCB interaction with soils is more dynamic than in the PAH model. A soil mass balance is created with inputs from atmospheric wet and dry deposition (in both the gas and particle phase) and losses from degradation, runoff, leaching, and re-volatilization to the atmosphere, meaning that the soil can either build up or become depleted of PCBs over time (in contrast to PAHs, which have a constant soil mass over time in GEOS-Chem). PCB cycling through the soil is calculated following a level III fugacity model¹², with fraction of organic carbon simulated using the Global Terrestrial Mercury Model (GTMM)¹³, which employs a version of the CASA biogeochemical model¹⁴ for carbon cycling. To build soil PCB mass over time, the model is spun up from 1930, when PCB emissions are first documented.

Meteorology The model is run from 1930 until 1997 using three consecutive years (2006-2008) of NASA GEOS5 reanalysis data repeatedly. Starting from 1997, all simulations are driven by output from the NASA GISS general circulation model, resolved at 3 or 6 h temporally, 4° latitude x 5° longitude, and 23 levels vertically. For present day (i.e., 2000) we use the means of 2001-2003, and for the future (i.e., 2050), we use the mean of 2051-2053 (with four years prior to each mean used to stabilize concentrations after the switch in meteorology). Future climate scenarios assume an SRES A1B scenario.

Emissions We use the global emissions inventory developed by Breivik et al.¹⁵ which includes emissions from various usages, disposals, and releases from the year 1930 until 2000. Breivik et al.¹⁵ also project future PCB emissions (2000-2100). For this study, after spin-up using year-dependent emissions, we use emissions from the year 2000 for all present-day climate scenarios, and from 2050 for all future climate scenarios. Emissions between 2000 and 2050 are not considered (for purposes of comparing to previous climate/emissions studies using the GEOS-Chem PAH model¹¹). Breivik et al. present "max", "default", and "min" scenarios for their inventory; here we use the "max" scenario given a better match to observations found in other studies⁶.

Results and discussion

Emissions Relative to the control scenario, primary emissions decline substantially in the FE scenario. FE emissions are only 0.01% and 0.04% of control emissions for CB28 and CB153, respectively. Declining primary

emissions and associated declines in atmospheric concentrations cause an increase in the percentage of secondary emissions. Percentage secondary emissions increase from 15% to nearly 100% for CB28, and from 3% to 98% for CB153. These increases result in declines of total emissions that are less drastic than declines in primary emissions: total FE emissions are 7% (CB28) and 2% (CB153) of control total emissions. In contrast, total emissions increase slightly in the FC scenario because of temperature-driven increases in secondary emissions (from 15% to 18% of total for CB28 and 3% to 4% for CB153). Emissions in the FCFE scenario are driven by the steep declines in FE, with total emissions increasing slightly compared to FE because of the increase from FC (total emissions are 8% and 3% of control total emissions for CB28 and CB153, respectively).

Concentrations Under FE, mean global concentrations decline for both CB28 and CB153, to 3% and 2% of those in the control, respectively, following declines in emissions (Figure 1). In the northern hemisphere, mid-latitude (5-60°N) concentrations also decline to 3% and 2% of control concentrations, while Arctic (60-90° N) concentrations are slightly lower (2% for CB28 and 0.3% for CB153). Despite small increases in total emissions, mean global concentrations decline slightly under FC as well (Figure 1), to 98% control levels for both congeners. In the northern hemisphere, mid-latitude results are similar to global average (concentrations are 100% and 98% control concentrations), but Arctic concentrations decrease further, to 91% and 90% those of the control. This is primarily because of greater losses via deposition and oxidation. The combined FCFE simulation results in global, mid-latitude, and Arctic mean concentration decreases similar to those seen under FE (Figure 1). For example, mean global concentrations decline to 4% (CB28) and 2% (CB153) of the control.

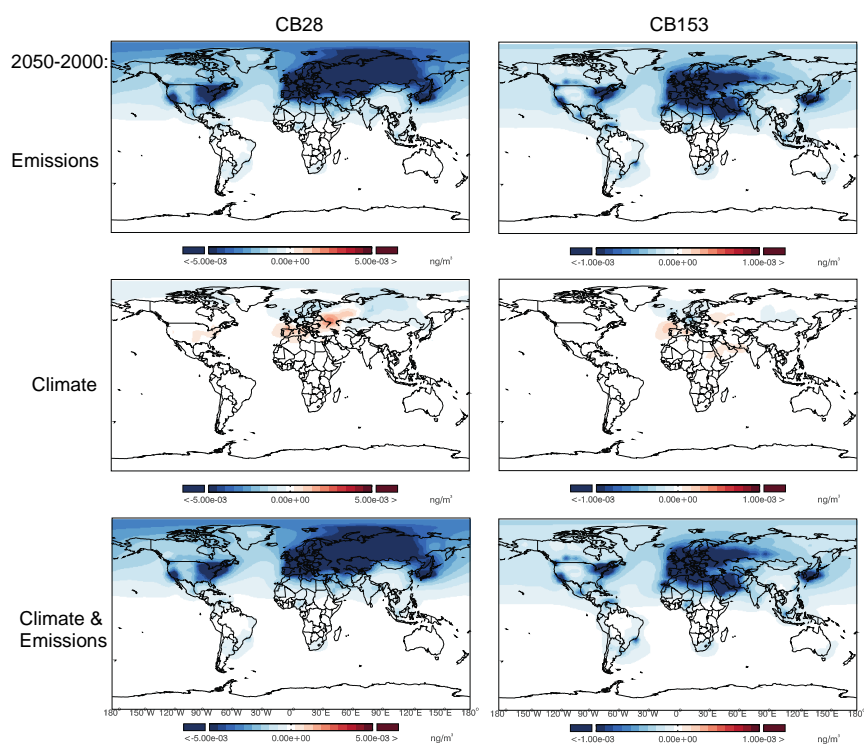


Figure 1. 2000-2050 changes in global CB28 and CB153 concentrations under emissions (top), climate (middle), and emissions and climate change combined (bottom) scenarios. Blue denotes a decrease; red denotes an increase.

Deposition In the control, total global deposition accounts for loss of 36% (CB28) and 73% (CB153) of emissions. Deposition normalized to emissions decreases for both PCBs in the FE scenario (by 5% and 37% for CB28 and CB153, respectively). Under the FC scenario, global deposition increases slightly for CB28 (by 2%)

but remains unchanged for CB153. The combined FCFE scenario is dominated by the changes seen under the FE scenario (normalized deposition goes down by 3% for CB28 and by 38% for CB153). For both PCBs, deposition changes are dominated by changes in gas phase dry deposition, which accounts for at least 98% of total deposition.

Oxidation In the control, oxidation accounts for 5% (CB28) and 2% (CB153) of loss of emissions. These values change by very little (<1%) in the FE, FC, and FCFE combined simulations. Sensitivity simulations using control OH concentrations indicate FC OH concentrations account for ~1% of the decline in Arctic concentrations under FC for both congeners.

Summary Our results suggest projected 2050 emissions will play a much stronger role than 2050 climate in controlling PCB concentrations of different volatilities. In our simulations, 2050 climate causes increases in emissions of only 4% at most (for the more volatile CB28), which does not impact concentrations substantially relative to 2050 emissions. Thus, the combined FCFE scenario is almost entirely dominated by changes from the FE scenario. Though PAH emissions are not projected to decline as substantially as with PCBs, our results are generally comparable to those determined under similar conditions for PAHs¹¹. There are several important caveats to these conclusions, however. Our simulations were conducted with soil-air interactions only; other surface-air interactions are known to be important for PCB cycling, and could have significant impacts especially on Arctic atmospheric concentrations. Also, in our model, only secondary emissions depend on temperature changes. Our FC and FE scenarios demonstrate that secondary emissions are more strongly impacted by the substantial decline in atmospheric concentrations under FE than they are by temperature changes under FC. Future work will address the impact of making primary emissions depend on temperature changes as well. Previous studies have found that the increase of primary passive volatilization emissions from temperature changes is the single most influential effect of future climate scenarios on modeled concentrations of CB28 and CB153⁶.

Acknowledgements

We thank Shiliang Wu (Michigan Technological University) and Eric Leibensperger (SUNY Plattsburgh) for assistance with GCM meteorology.

References:

1. Wania F, Mackay D (1993); *Ambio* 22: 10-18.
2. Hung H, Lee SC, Wania F, Blanchard P, Brice K (2005); *Atmos. Environ.* 39: 6502-6512.
3. MacLeod M, Riley WJ, McKone TE (2005); *Environ. Sci. Technol.* 39: 6749-6756.
4. Gong SL, Huang P, Zhao TL, Sahsuvar L, Barrie LA, Kaminski JW, Li YF, Niu T (2007); *Atmos. Chem. Phys.* 7: 4001-4013.
5. Huang P, Gong SL, Zhao TL, Neary L, Barrie LA (2007); *Atmos. Chem. Phys.* 7: 4015-4025.
6. Lamon L, von Waldow H, MacLeod M, Scheringer M, Marcomini A, Hungerbuhler K. (2009); *Environ. Sci. Technol.* 43: 5818-5824.
7. Ma J, Cao Z (2010); *Environ. Sci. Technol.* 44: 8567-8573.
8. Ma J, Hung H, Tian C, Kallenborn R (2011); *Nature Clim. Change* 1: 255-260.
9. Bey I, Jacob DJ, Yantosca RM, Logan JA, Field B, Fiore AM, Li Q, Liu HX, Mickley LJ, Schultz M (2001); *J. Geophys. Res.* 106: 23,073-23,096.
10. Friedman CL, Selin NE (2012); *Environ. Sci. Technol.* 46: 9501-9510.
11. Friedman CL, Zhang Y, Selin NE (2014); *Environ. Sci. Technol.* 48: 429-437.
12. Mackay D, Paterson S (1991); *Environ. Sci. Technol.* 25: 427-436.
13. Smith-Downey N, Sunderland E, Jacob D (2010); *J. Geophys. Res.* 115: G03008.
14. Potter CS, Randerson JT, Field CB, Matson PA, Vitousek PM, Mooney HA, Klooster SA (1993); *Global Biogeochem. Cycles* 7: 811-841.
15. Breivik, K, Sweetman A, Pacyna JM, Jones KC (2007); *Sci. Total Environ.* 377: 296-307.